IOSR Journal of Engineering (IOSRJEN) **www.iosrjen.org**
ISSN (e): 2250-3021, ISSN (p): 2278-8719
Vol. 11, Issue 5, May 2021, ||Series -II|| PP 01-05

Active Control of Graphene-Reinforced Nanocomposite Beams under Damped Time-Delay Feedback

Zhang Hui, Feng Qin
(Department of mechanical and electrical engineering, Dazhou Vocational and Technial College, China)
Received 08 May 2021; Accepted 23 May 2021

ABSTRACT: Based on the Halpin-Tsai approximate physical property model, using the von-Karman strain-displacement relationship, the governing equations of the graphene composite beam under damped time-delay are established. The Galerkin method is used to decouple and solve the equation. The linear stability region of the system under active control is analyzed theoretically. It is found that the area of the stability region gradually decreases with the increase of time delay, and the number of stability regions is finally reduced from theoretical n to one with the increase of control gain. The nonlinear numerical calculation gives the bifurcation response of the nonlinear system with time-delay, and it can very well confirm the theoretical results.
KEYWORDS: Graphene; Nanocomposites; The first-order shear deformation beam theory; Active control; Stability

I. INTRODUCTION

Graphene is currently the thinnest two-dimensional material found in the world and has superior mechanical properties. Its theoretical strength can reach 125 GPa, which is 100 times of that of steel; its elastic modulus is 1.0 TPa, which is comparable to carbon nanotubes [1,2]. Graphene therefore becomes an ideal reinforcement material for nanocomposites. Due to the physical properties of high strength, high stiffness and low density, graphene nanocomposites are expected to be used to develop key structures in the fields of civil engineering, aerospace, etc [3].

When an aerospace structure is operating in space, once it is excited by some kind of excitation, its vibration will continue for a long time, which will seriously affect the stability and accuracy of the structure. Therefore, the vibration control of the structure has very important engineering significance. From the perspective of dynamic control, there are mainly two methods: active control and passive control. Since the active control does not rely on external excitation, its control effect is significantly better than passive control.

Therefore, in order to explore the active control effect of graphene nanocomposite beams, a damping time delay term is introduced to better fit the actual process. The physical parameters of the structure are given by the Halpin-Tsai model [4]. Based on the von Karman strain-displacement relationship [5], the governing equations of the beam are established, and the equations are solved by the Galerkin method. The linear stability region of the beam with specific volume fraction is analyzed theoretically, and the bifurcation diagram of the nonlinear system is given through numerical calculation, and the comparison shows that it can very well confirm the theoretical results. Finally, in order to explain the nonlinear vibration state more intuitively, we give the time history curves and phase graph of the structure under the control of several groups of special parameters.

Ⅰ. Material parameters

Assuming that graphene nanosheets are randomly distributed in the matrix material, according to the Halpin-Tsai micromechanical model [4], the elastic modulus of graphene nanocomposites is as follows:

$$E_C = \frac{3}{8}\frac{1+(2L_G/3T_G)\eta_L V_G}{1-\eta_L V_G}\times E_M + \frac{5}{8}\frac{1+2\eta_W V_G}{1-\eta_W V_G}\times E_M \tag{1}$$

Where

$$\eta_L = \frac{(E_G/E_M)-1}{E_G/E_M+2L_G/3T_G},\quad \eta_W = \frac{(E_G/E_M)-1}{E_G/E_M+2}$$

Where L_G and T_G are the average length and thickness of the graphene nanosheets, V_G is the volume fraction of the graphene nanosheets, and E_G and E_M are the elastic modulus of the graphene nanosheets and the matrix material, respectively. The density and Poisson's ratio of graphene nanocomposites can be estimated can be estimated by the mixing law:

$$\rho_C = \rho_G V_G + \rho_M V_M \tag{2a}$$

$$\nu_C = \nu_C V_G + \nu_M V_M \tag{2b}$$

In the formula, the subscripts C, G and M represent composite materials, grapheme nanosheets and matrix materials, respectively.

Ⅱ. Vibration control equation

Using von Karman strain-displacement relationship [5,6]:

$$\varepsilon_x = \frac{\partial u}{\partial x} + z\frac{\partial \phi}{\partial x} + \frac{1}{2}\left(\frac{\partial w}{\partial x}\right)^2 \tag{3a}$$

$$\gamma_{xz} = \frac{\partial w}{\partial x} + \phi \tag{3b}$$

The strain energy of the beam can be expressed as:

$$U = \frac{1}{2}\int_0^l \int_{-\frac{h}{2}}^{\frac{h}{2}} \left[E_C \left(\frac{\partial u}{\partial x} + z\frac{\partial \phi}{\partial x} + \frac{1}{2}\left(\frac{\partial w}{\partial x}\right)^2 \right)^2 + G_C \left(\frac{\partial w}{\partial x} + \phi \right)^2 \right] \mathrm{d}z\mathrm{d}x \tag{4}$$

In the formula, u、ϕ and w represent the beam's axial displacement, cross-sectional rotation angle and transverse displacement, respectively. The kinetic energy of the beam can be expressed as

$$K = \frac{\rho_C}{2}\int_0^l \int_{-\frac{h}{2}}^{\frac{h}{2}} \left[\left(\frac{\partial u}{\partial t} + z\frac{\partial \phi}{\partial t} \right)^2 + \left(\frac{\partial w}{\partial t} \right)^2 \right] \mathrm{d}x\mathrm{d}z \tag{5}$$

The work done by the external force is

$$\Theta = \int_0^l \left[\int_{-\frac{h}{2}}^{\frac{h}{2}} \rho_C \left(f_x u + f_z w \right)\mathrm{d}z + \left(-\int_0^w \left(c\frac{\partial w}{\partial x} \right)\mathrm{d}w \right) \right] \mathrm{d}x \tag{6}$$

Where f_x and f_z represent the volume force in the x and z directions, respectively, and c is the damping coefficient.

According to Hamilton's principle: $\delta\int_{t_1}^{t_2}(K - U + \Theta)\mathrm{d}t = 0$, Without considering the work done by volume force and ignoring the axial displacement, the nonlinear vibration equation of the beam in damping state can be obtained:

$$\frac{3}{2}C\left(\frac{\partial w}{\partial x}\right)^2\frac{\partial^2 w}{\partial x^2} + C_{55}\left(\frac{\partial^2 w}{\partial x^2} + \frac{\partial \phi}{\partial x}\right) = I_0\frac{\partial^2 w}{\partial t^2} + c\frac{\partial w}{\partial t} \tag{7a}$$

$$D\frac{\partial^2 \phi}{\partial x^2} - C_{55}\left(\frac{\partial w}{\partial x} + \phi\right) = I_1\frac{\partial^2 \phi}{\partial t^2} \tag{7b}$$

In equation (7), the coefficients of stiffness and inertia are as follows:

$$\{C, D\} = \int_{-\frac{h}{2}}^{\frac{h}{2}} E_C \{1, z^2\}\mathrm{d}z \;,\; \{I_0, I_1\} = \int_{-\frac{h}{2}}^{\frac{h}{2}} \rho_C \{1, z^2\}\mathrm{d}z \;,\; C_{55} = \int_{-\frac{h}{2}}^{\frac{h}{2}} G_C \mathrm{d}z \tag{8}$$

Ⅲ. Linear stability analysis

Introduce the following dimensionless quantities:

$$X = x/l,\; W = w/h,\; \bar{t} = t\sqrt{G_C/(\rho_C h^2)},\; \bar{c} = c/\sqrt{G_C \rho_C},\; \zeta = E_C/G_C,\; \lambda = h/l$$

Then the governing equation (7) can be dimensionless:

$$\lambda^2\frac{\partial^2 W}{\partial X^2} + \lambda\frac{\partial \phi}{\partial X} + \frac{3}{2}\zeta\lambda^4\left(\frac{\partial W}{\partial X}\right)^2\frac{\partial^2 W}{\partial X^2} = \frac{\partial^2 W}{\partial \bar{t}^2} + c\frac{\partial W}{\partial \bar{t}} \tag{9a}$$

$$\zeta\lambda^2\frac{\partial^2 \phi}{\partial X^2} - 12\left(\lambda\frac{\partial W}{\partial X} + \phi\right) = \frac{\partial^2 \phi}{\partial \bar{t}^2} \tag{9b}$$

In order to obtain the approximate solution of equation (9), the Galerkin method is used to discretize it. Let the first-order approximate solution be:

$$\begin{cases} W(X, \bar{t}) = \sin(\pi X) S_1(\bar{t}) \\ \phi(X, \bar{t}) = \cos(\pi X) S_2(\bar{t}) \end{cases} \tag{10}$$

Substituting equation (10) into equation (9), and integrating in the X direction, while introducing the time-delay damping term, we get:

$$\ddot{S}_1 + k\bar{c}\dot{S}_1(\bar{t}-\tau) + \lambda^2\pi^2 S_1 + \lambda\pi S_2 + \frac{3}{4}\zeta\lambda^4\pi^4 S_1^3 = 0 \tag{11a}$$

$$\ddot{S}_2 + \zeta\lambda^2\pi^2 S_2 + \lambda\pi S_2 + 12(\lambda\pi S_1 + S_2) = 0 \tag{11b}$$

Where k is the control gain and τ is the time delay. In order to analyze the linear stability region of the system , suppose the solution of the system is:

$$\begin{cases} S_1(\bar{t}) = E\cdot\exp(\beta + i\omega\bar{t}) \\ S_2(\bar{t}) = D\cdot\exp(\beta + i\omega\bar{t}) \end{cases} \tag{12}$$

Then equation (11) becomes:

$$Er^2 + E\lambda^2\pi^2 + D\lambda\pi + Ek\bar{c}r\cdot\exp(-r\tau) = 0 \tag{13a}$$

$$Dr^2 + D\zeta\lambda^2\pi^2 + 12E\lambda\pi + 12D = 0 \tag{13b}$$

In equation (13), $r = \beta + i\omega t$. For the system to have a non-zero solution, the following conditions must be satisfied:

$$\begin{vmatrix} r^2 + \lambda^2\pi^2 + \bar{k}r\cdot\exp(-r\tau) & \lambda\pi \\ 12\lambda\pi & r^2 + \zeta\lambda^2\pi^2 + 12 \end{vmatrix} = 0 \tag{14}$$

Where $\bar{k} = k\bar{c}$. For a linear system, when $\beta < 0$, the system is stable; when $\beta > 0$, the system is unstable. In order to obtain the boundary between the stable and unstable solutions of the system, let $\beta = 0$, that is, $r = i\omega t$, then according to equation (14), we can get:

$$\left(-\omega^2 + \lambda^2\pi^2 + i\bar{k}\omega\exp(-i\omega\tau)\right)\cdot\left(-\omega^2 + \zeta\lambda^2\pi^2 + 12\right) - 12\lambda^2\pi^2 = 0 \tag{15}$$

Separating the real and imaginary parts in equation (15), we can get:

$$\bar{k}\omega\left(-\omega^2 + \zeta\lambda^2\pi^2 + 12\right)\cdot\cos(\omega\tau) = 0 \tag{16a}$$

$$\bar{k}\omega\left(-\omega^2 + \zeta\lambda^2\pi^2 + 12\right)\cdot\sin(\omega\tau) = -\omega^4 + \left(\lambda^2\pi^2 + \zeta\lambda^2\pi^2 + 12\right)\cdot\omega^2 - \zeta\lambda^4\pi^4 \tag{16b}$$

By solving equation (16), we can get

$$\tau = \frac{2j\pi + \pi}{2\omega}, \quad j = 0,1,2,\cdots \tag{17a}$$

$$\bar{k} = \frac{(-1)^{j+1}\left[\omega^4 - \left(\lambda^2\pi^2 + \zeta\lambda^2\pi^2 + 12\right)\cdot\omega^2 + \zeta\lambda^4\pi^4\right]}{\omega\left(-\omega^2 + \zeta\lambda^2\pi^2 + 12\right)}, \quad j = 0,1,2,\ldots \tag{17b}$$

It can be seen from equation (17) that the stability of the beam solution can be achieved by controlling the time delay τ and the gain coefficient $\bar{k}$.

Ⅳ. Numerical calculation and analysis

Consider the graphene nanosheet/epoxy nanocomposite beam, set $\lambda = 1/5$ and $V_G = 0.5\%$, and the material parameters are shown in Table 1.

Table 1 GPL and epoxy resin properties

Material parameters	Graphene nanosheets [7]	Epoxy resin [8]
Average thickness (nm)	0.8[9]	/
Average length (μm)	1[9]	/
Elastic Modulus (GPa)	1010	3.0
Density (kg/m^{-3})	1062.5	1200
Poisson's ratio	0.186[10]	0.34

According to formula (18), the stability solution of the linear system can be calculated., as shown in Figure 1 .The shaded part in the figure represents the stable area of the system, that is, its internal parameters $(\bar{k},\tau)$ can ensure that the control system can return to the equilibrium position under any small disturbance. In addition, it is found that with the increase of time delay τ, the area of stability region decreases obviously, and as gain coefficient k increases, the number of stability region of the system decreases from theoretically multiple to one, that is, when $\bar{k}$ is a fixed value, the stability of the system changes with the time delay: when $\bar{k} < -0.206$, there is no stability region; when $\bar{k} \in (-0.206, 0)$, the system has at least one stability region; when $\bar{k} \in (0, 0.044)$, There are at least 3 stability region; when $\bar{k} \in (0.044, 0.21)$, the system has 2 stable regions; when $\bar{k} > 0.21$, the system has only one stability region.

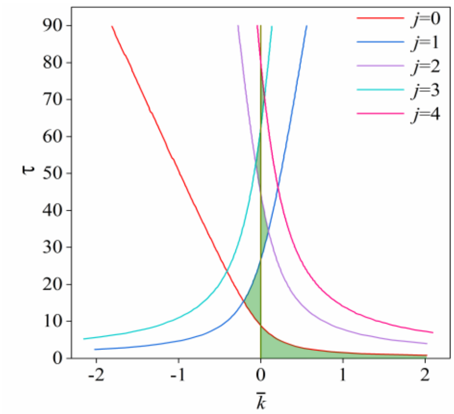

Figure 1 The stability region of the solution

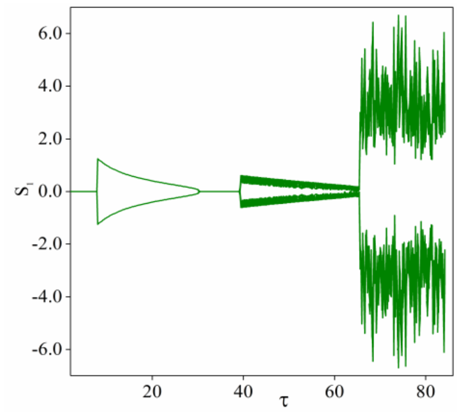

Figure 2 Bifurcation diagram

Set $\dot{S}_i = 0 (i = 1, 2)$ to solve the nonlinear control equation (11). Figure 2 shows the bifurcation diagram of the beam when the control gain coefficient $\bar{k} = 0.05$, The figure clearly reflects that when the control gain coefficient $\bar{k} = 0.05 \in (0.044, 0.21)$, there are only two stable regions in the system, namely $\tau \in (0, 7.8)$ and $\tau \in (30.4, 38.8)$ .Compared with figure 1, it is found that the theoretical results are well confirmed. when $\tau \in (7.8, 30.4)$, the system enters into a single periodic motion when it loses stability for the first time; when $\tau > 38.8$, the system goes from the second steady state to multi period motion and chaos. Therefore, when the control gain coefficient and time delay of the system are in the shaded part in Fig. 1, the system can achieve a good active control effect.

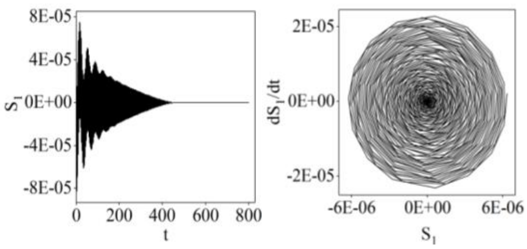

Figure 3 $\tau = 0.01$, the time history curves and phase graph

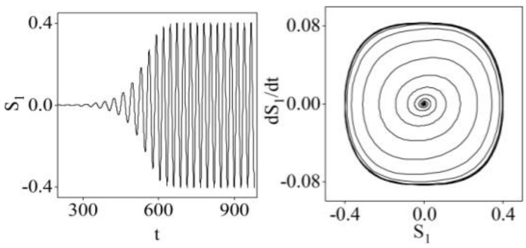

Figure 4 $\tau = 20$, the time history curves and phase graph

Figures 3 to 6 show the time history curves and phase graph when the values of time delay τ are 0.01, 20, 52.8, and 70, respectively, where $\bar{k}$ is 0.05. It can be seen from Figure 3 that the system is in the steady state zone of the first stage when $\tau = 0.01$, that is, once the system vibrates due to external excitation, it can self-adjust to a balanced state; When the system loses stability for the first time, it enters a periodic motion state. Here we give the single-period response graph of the system when $\tau = 20$, that is, when the system is subjected to small disturbances, it cannot enter equilibrium eventually, but presents periodic motion after a period of irregular vibration, as shown in Figure 4; when the system loses stability for the second time, it enters multiple periodic motions and chaos, For example, when $\tau = 52.8$, The system presents a 7 times period response, as shown in Figure 5; when $\tau = 70$, it shows a chaotic state, as shown in Figure 6.

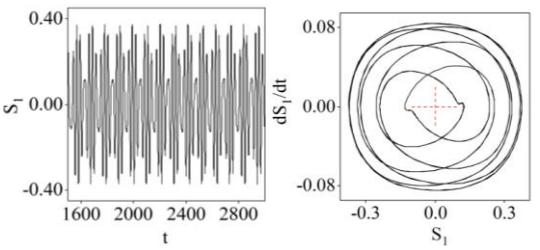

Figure5 $\tau = 52.8$, the time history curves and phase graph

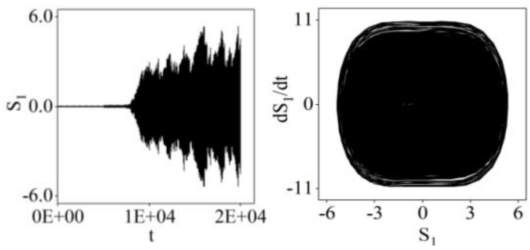

Figure6 $\tau = 70$, the time history curves and phase graph

II. CONCLUSION

Based on von Karman strain displacement relationship and Halpin Tsai physical parameter model, the governing equations of graphene nanocomposite beam with time-delay feedback are established.Through theoretical and numerical analysis, the active control effect of the control system is studied. The results show that by properly adjusting the parameters of the system, the disturbed structure can quickly return to the stable state, and when the system parameters are in the unstable region, the vibration form of the structure show single period motion, multiple period motion and chaos, these vibration forms will affect the structure's stability and working accuracy in space, and need to be avoided as much as possible. Finally, it needs to be pointed out that although this article describes the active control effect of graphene nanocomposite beams from both theoretical and numerical aspects, how to apply it in engineering is still a subject that requires a lot of research.

REFERENCE:

[1]. Balandin A A, Ghosh S, Bao W, et al. Superior thermal conductivity of single-layer graphene [J]. Nano Letters, 2008, 8(3): 902.
[2]. Du X, Skachko I, Barker A, et al. Approaching ballistic transport in suspended graphene [J]. Nature Nanotechnology, 2008, 3(8): 491-5.
[3]. Wu H, Yang J, Kitipornchai S. Dynamic instability of functionally graded multilayer graphene nanocomposite beams in thermal environment [J]. Composite Structures, 2017, 162(1):244-54.
[4]. Affdl J C H, Kardos J L. The Halpin‐Tsai equations: A review [J]. Polymer Engineering & Science, 1976, 16(5): 344–52.
[5]. Asghari M, Kahrobaiyan M H, Ahmadian M T. A nonlinear Timoshenko beam formulation based on the modified couple stress theory [J]. International Journal of Engineering Science, 2010, 48(12): 1749-61.
[6]. Huang T, Lu R, Su C, et al. Chemically modified graphene/polyimide composite films based on utilization of covalent bonding and oriented distribution [J]. Acs Appl Mater Interfaces, 2012, 4(5): 2699-708.
[7]. Rafiee M A, Rafiee J, Wang Z, et al. Enhanced Mechanical Properties of Nanocomposites at Low Graphene Content [J]. Acs Nano, 2009, 3(12): 3884.
[8]. He B, Wang X. ERROR ANALYSIS IN DIFFERENTIAL QUADRATURE METHOD [J]. Transactions of Nanjing University of Aeronautics and Astronautics, 1994, 2): 194-200.
[9]. Zhao X, Zhang Q, Chen D, et al. Enhanced Mechanical Properties of Graphene-Based Poly(vinyl alcohol) Composites [J]. Macromolecules, 2010, 43(5): 2357-63.
[10]. Liu F, Ming P, Li J. Ab initio calculation of ideal strength and phonon instability of graphene under tension [J]. Physrevb, 2007, 76(6): 471-8.

Zhang Hui, et. al. "Active Control of Graphene-Reinforced Nanocomposite Beams Under Damped Time-Delay Feedback." *IOSR Journal of Engineering (IOSRJEN)*, 11(05), 2021, pp. 01-05.